

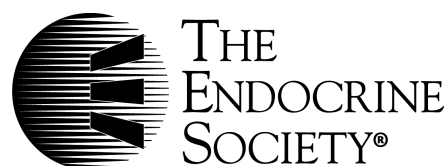
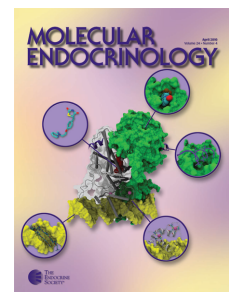
Endocrinology

Characterization of Voltage-Gated Calcium Currents in Gonadotropin-Releasing Hormone Neurons Tagged with Green Fluorescent Protein in Rats

Masakatsu Kato, Kumiko Ui-Tei, Miho Watanabe and Yasuo Sakuma

Endocrinology 2003 144:5118-5125 originally published online Aug 13, 2003; , doi: 10.1210/en.2003-0213

To subscribe to *Endocrinology* or any of the other journals published by The Endocrine Society please go to: <http://endo.endojournals.org//subscriptions/>



Characterization of Voltage-Gated Calcium Currents in Gonadotropin-Releasing Hormone Neurons Tagged with Green Fluorescent Protein in Rats

MASAKATSU KATO, KUMIKO UI-TEI, MIHO WATANABE, AND YASUO SAKUMA

Department of Physiology, Nippon Medical School (M.K., M.W., Y.S.), Tokyo 113-8602, Japan; and Department of Biophysics and Biochemistry, School of Science, University of Tokyo (K.U.-T.), Tokyo 113-0033, Japan

Functional analysis of GnRH neurons is limited, although these neurons play an important role in neuroendocrine regulation. Therefore, we decided to conduct cell physiological analysis of GnRH neurons. To identify GnRH neurons, we tagged the neurons with green fluorescence protein by a transgenic technique. A dispersed culture of GnRH neurons was prepared from the transgenic rats. After overnight culture, a perforated patch clamp was applied to the identified GnRH neurons to analyze the Ca^{2+} currents. In neonatal GnRH neurons, high voltage-activated Ca^{2+} currents were clearly observed, but low voltage-activated Ca^{2+} current was negligible. Nimodipine (L-type channel blocker) and ω -conotoxin GVIA (N-type channel blocker) each attenuated the cur-

rent by approximately 20%. The R-type channel blocker SNX-482 attenuated the current by approximately 55%. Inhibition by the P/Q-type channel blocker ω -agatoxin IVA was small. In GnRH neurons around puberty, however, both high and low voltage-activated Ca^{2+} currents were observed. Inhibitions by nifedipine, ω -conotoxin GVIA, and SNX-482 were similar to those in the neonatal neurons, whereas the inhibition by ω -agatoxin IVA was clearly seen in 40–61% of the GnRH neurons examined. These results indicate that GnRH neurons functionally express L-, N-, P/Q-, R-, and T-type channels. Expressions of P/Q- and T-type channels are developmentally regulated. (*Endocrinology* 144: 5118–5125, 2003)

GnRH NEURONS PLAY an essential role in reproductive neuroendocrine regulation. Despite the importance of GnRH neurons, functional analysis of these neurons is limited. This is mainly due to difficulty in identifying GnRH neurons in electrophysiological experiments. Recently, however, transgenic mice were produced for specific labeling of GnRH neurons with enhanced green fluorescence protein (EGFP) (1–3), which has facilitated the cell physiological study of GnRH neurons. Firing patterns of GnRH neurons were studied in whole cell patch-clamp recordings (2, 4, 5), and the basic membrane properties were studied in current clamp analysis (3). Responses to glutamate and γ -aminobutyric acid were also reported on EGFP-tagged GnRH neurons (1, 5, 6). Because most of these studies were carried out in the current clamp mode, the voltage-gated currents remain to be analyzed. Kusano *et al.* (7) reported that mouse GnRH neurons in olfactory pit explant cultures express both low voltage-activated and high voltage activated Ca^{2+} currents. This report is to date the only one on the voltage-gated Ca^{2+} current in GnRH neurons analyzed by the voltage clamp experiments despite the fact that the voltage-gated Ca^{2+} channels play important roles in Ca^{2+} -dependent cellular functions such as transmitter release, cell excitability, protein phosphorylation, enzyme activity, and gene transcription. We therefore decided to study the voltage-gated Ca^{2+} currents in rat GnRH neurons. We first produced transgenic rats for the identification of GnRH neurons.

Here are two reasons why we chose rats instead of mice. First, there are already several mouse lines of EGFP-tagged GnRH neurons. If we produced a transgenic rat, we could compare GnRH neurons in mice and rats. Second, rats have been and are still commonly used for experiments on reproductive neuroendocrinology, as a consequence of which there is an accumulation of useful data on rats.

In the present study we investigated the expression profile of voltage-gated Ca^{2+} currents in neonatal and pubertal GnRH neurons by the method of perforated patch recording configuration with amphotericin B.

Materials and Methods

All experiments were performed with the approval of Nippon Medical School animal care committee.

Transgenic rats

The rat GnRH promoter (–3026 to +116; a gift from Dr. M. E. Wierman, University of Colorado Health Science Center, Denver, CO) (8) was used to express a transgene consisting of the intron of rabbit β -globin (640 bp; a gift from Dr. J. Miyazaki, Osaka University, Osaka, Japan), the coding sequence for EGFP (739 bp; CLONTECH Laboratories, Inc., Tokyo, Japan), and the polyadenylation signal. The excised transgene was injected into the pronucleus of fertilized oocytes obtained from Wistar rats (YS New Technology, Tochigi, Japan). Six transgenic founders were identified through Southern blot analysis of DNA harvested from tail snips of 112 pups with a ^{32}P -labeled EGFP probe. The offspring of these 6 transgenic lines were cytologically examined, and one transgenic line, which had high and specific expression of EGFP in GnRH neurons, was selected for physiological experiments. The other five lines were not used because they had weak EGFP fluorescence. For cytological observation, brains were fixed with 4% paraformaldehyde. Forty-micrometer frozen sections of the fixed brain were cut and immunostained with antisera to GnRH (a gift from Dr. K. Inoue, Saitama

Abbreviations: Aga-IVA, ω -Agatoxin IVA; APW, action potential waveform; EGFP, enhanced green fluorescence protein; GVIA, ω -conotoxin GVIA; MVIIC, ω -conotoxin MVIIC; OVLT, organum vasculosum of the lamina terminalis.

University, Saitama, Japan) and Cy3-labeled second antibody (Jackson ImmunoResearch Laboratories, West Grove, PA).

Primary culture

The brains were excised from either 1- to 7-d-old pups or 35- to 40-d-old rats under ether anesthesia. The former were used to prepare neonatal neurons, and the latter were used for the neurons around puberty. The latter could include prepubertal animals because we did not check for the onset of puberty. Medial septum, diagonal band of Broca, organum vasculosum of the lamina terminalis (OVLT), and medial preoptic area were cut out with a razor and surgical blades. The sections were minced and treated with papain (21 U/ml; Funakoshi, Tokyo, Japan) for 30–60 min at 30°C with gentle agitation. The tissues were triturated with a 5-ml plastic pipette after several washes with MEM (Life Technologies, Inc., Tokyo, Japan). The cell suspension was applied to discontinuous Percoll density gradient centrifugation to remove debris. The cells were obtained from the middle layer of the density gradient centrifugation composed of 1.0, 1.023, and 1.078 g/ml layers and were plated on poly-lysine-coated coverslips and incubated overnight in Neurobasal-A medium (Life Technologies, Inc.) supplemented with 0.5 mM L-glutamine and B-27 (Life Technologies, Inc.) at 37°C. Most of the dissociated GnRH neurons were round, but some were spindle-shaped. These neurons did not change their shape during the overnight culture.

Electrophysiology

The List EPC-9 patch-clamp system (Physio-Tech, Tokyo, Japan) was used for electrophysiological recordings and data analysis. Whole cell currents were measured by the perforated patch-clamp technique (9) at room temperature (25°C). The final concentration of amphotericin B (Seikagaku Corp., Tokyo, Japan) in the pipette solution was 0.05 mg/ml. The pipette solution consisted of 95 mM cesium aspartate, 47.5 mM CsCl, 1.0 mM MgCl₂, 0.1 mM EGTA, and 10 mM HEPES (pH 7.2), and the osmolality was adjusted to 270 mosmol. The extracellular solution consisted of 116.3 mM NaCl, 10 mM tetraethylammonium chloride, 5 mM CsCl, 10 mM CaCl₂, 0.8 mM MgCl₂, 0.6 mM NaHCO₃, 10 mM glucose, 20 mM HEPES (pH 7.4), 0.1% BSA (fraction V, Sigma-Aldrich Corp., St. Louis, MO), and 0.3 μM TTX (Seikagaku Corp.), and the osmolality was adjusted to 300 mosmol. Pipettes were fabricated with borosilicate glass capillaries and had a resistance of 7–9 MΩ. The pipettes were targeted to GnRH neurons in the extracellular solution without BSA. After touching the cell, slight negative pressure was applied to the pipette, which made a seal resistance of 5–10 GΩ. Perforation with amphotericin B was achieved within 5–10 min after giga-seal formation. Currents were filtered at 2.3 kHz, digitized at 10 kHz, and recorded. Series resistance was 70% electronically compensated. Data were taken when the series resistance was stable and less than 30 MΩ. Capacitive and leak currents were subtracted by the p/4 protocol, and the liquid junction potential was not compensated. Cell capacitances were 9.2 ± 2.2 pF (n = 46) in males and 9.8 ± 2.4 pF (n = 34) in females in neonates, and 12.8 ± 2.6 pF (n = 13) in males and 10.8 ± 2.7 pF (n = 11) in females around puberty. The input resistance of the cells ranged from 1–5 GΩ. Cells with a peak Ca²⁺ current less than –100 pA were excluded from the analysis, because it is difficult to obtain a reliable subtracted current with such small currents. To confirm the perforated patch configuration, we examined the capacitive current and its change by rupturing the patch membrane at the end of the recording. Data are expressed as the mean ± SD unless otherwise stated. The Kruskal-Wallis test and paired *t* test were used for statistical analysis. The significance level was set at *P* < 0.05.

Chemicals

Nimodipine and nifedipine were obtained from Wako Junyaku (Osaka, Japan). ω-Conotoxin GVIA (GVIA), ω-conotoxin MVIIC (MVIIC), ω-agatoxin IVA (Aga-IVA), and SNX-482 were purchased from Peptide Institute, Inc. (Osaka, Japan).

Results

In the transgenic rats, EGFP fluorescence was observed only in GnRH-immunoreactive neurons, approximately one

third of which had strong EGFP fluorescence (Fig. 1). The fluorescence was observed not only in soma, but also in processes including axons in the median eminence (data not shown). GnRH neurons were also identified with EGFP in a dissociated culture (Fig. 1, D–F).

Ca²⁺ currents in neonatal GnRH neurons

In neonatal GnRH neurons Ca²⁺ currents were activated by 100-msec voltage steps from –60 to 60 mV in 10-mV increments from a holding potential of –80 mV at 0.2 Hz (Fig. 2). The maximum amplitudes were –57.8 ± 20.7 pA/pF (n = 13) in males and –46.6 ± 12.2 pA/pF (n = 14) in females. The maximum current was activated at 0–20 mV and showed a rapid activation and a relatively slow inactivation.

The effects of several Ca²⁺ channel blockers on the maximum currents are shown in Fig. 3. The maximum currents were elicited by 100-msec voltage pulses to 0 or 10 mV from the holding potential of –80 mV at 0.2 Hz. After the control currents were recorded, 10 μM nimodipine, 1 μM GVIA, 200 nM Aga-IVA, and 100 nM SNX-482 were successively applied (Fig. 3, A and B). The initial peak currents and late sustained currents were examined. In the initial peak currents, nimodipine and GVIA each attenuated the currents by approximately 20%, and SNX-482 reduced the currents by about 55% in both sexes. A similar inhibition by SNX-482 (60 ± 7%; n = 4) was observed when SNX-482 was applied without prior application of the other Ca²⁺ channel blockers. Inhibition by Aga-IVA was small and negligible in both sexes. Aga-IVA exerted 7.5 ± 3.3% inhibition in 4 of 11 male cells examined and 3% inhibition in 1 of 14 female cells examined. No inhibition was observed in other cells. After combined application of all the above drugs, 6–7% of the control current remained. To examine the presence of T-type Ca²⁺ current, the membrane potential was held at –100 mV, and the voltage steps to –70, –60, and –50 mV were given at 0.2 Hz. In this voltage protocol the current density of –1 pA/pF was activated at –50 mV in 2 cells among 10 male cells examined, and that of –1.4 pA/pF was activated at –50 mV in 3 cells among 9 female cells examined (Fig. 7C). No current was activated at –50 mV in the other cells. In the late sustained currents, the inhibition caused by GVIA was approximately 30%, and that by SNX-482 was 33% in males and 47% in females. The proportion of SNX-482-sensitive currents was smaller in the late sustained currents than in the initial peak currents. This is probably due to inactivation of the SNX-482-sensitive currents. The inhibition by each blocker was significant (*P* < 0.01), except for that by Aga-IVA.

The action potential waveform (APW) was used for activation of the Ca²⁺ currents (Fig. 4). The half-amplitude width of APW was set at 2.5 msec, because that of the GnRH neuron ranged from 2.5–3 msec at room temperature (data not shown). In this voltage protocol, the inhibitory effect of nifedipine was small (9.4%), and the inhibition caused by GVIA and Aga-IVA was 29%, whereas that by SNX-482 was 45%, so that the contribution of the nifedipine-sensitive current was smaller in the APW than in the current activated by the square pulse.

The voltage-dependent activation of R-type current was studied by measuring tail currents at –80 mV after 10-msec

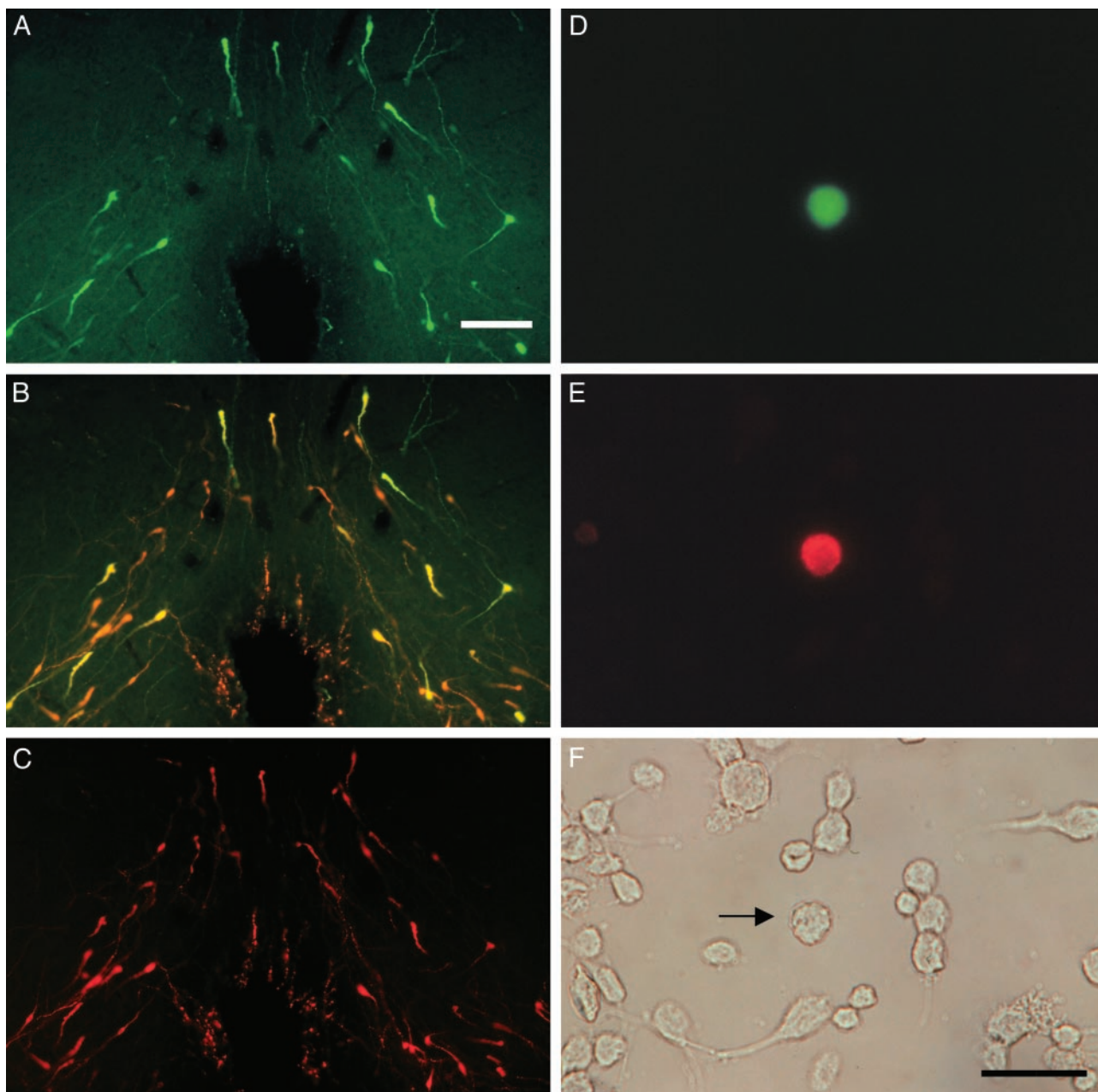


FIG. 1. EGFP fluorescence in GnRH neurons. A–C, Frontal section of the OVLT, diagonal band of Broca region. The dark area in the lower middle of each panel is the rostral part of the third ventricle. A, EGFP fluorescence. B, Double exposure for EGFP and Cy3 (GnRH). Neurons colored yellow are positive for both EGFP and GnRH. C, Cy3-labeled GnRH neurons. D–F, Dissociated cells, D, EGFP fluorescence. E, Cy-3-labeled GnRH neuron. F, Cells in brightfield. The cell indicated with an arrow is the EGFP-positive GnRH neuron. Scale bars, 100 μm (A) and 25 μm (F).

prepulses of -60 to 60 mV in 10 -mV increments from the holding potential of -80 mV at 0.2 Hz in the presence of nimodipine, GVIA, and Aga-IVA (Fig. 5). The activation started at a prepulse of -40 mV and reached full activation at 30 – 40 mV. The half-activation voltage was 0 mV (two male and two female neurons). Steady state inactivation was also studied in the R-type Ca^{2+} current (Fig. 5). The holding potential varied from -100 to 0 mV in 10 -mV increments, and a 100 -ms test pulse was applied at 0.2 Hz. The inactivation started from the holding potential of -80 mV and reached almost complete inactivation at 0 mV. The half-

inactivation voltage was -39 mV (seven male and three female neurons).

Ca^{2+} currents in GnRH neurons around puberty

Ca^{2+} currents were activated by 100 -msec voltage steps from -60 to 60 mV in 10 -mV increments from the holding potential of -80 mV at 0.2 Hz. The activation started at -40 mV and reached maximum amplitude around 0 mV. The maximum amplitudes were -49.5 ± 15.1 pA/pF ($n = 13$) in males and -43.9 ± 26.8 pA/pF ($n = 10$) in females. The

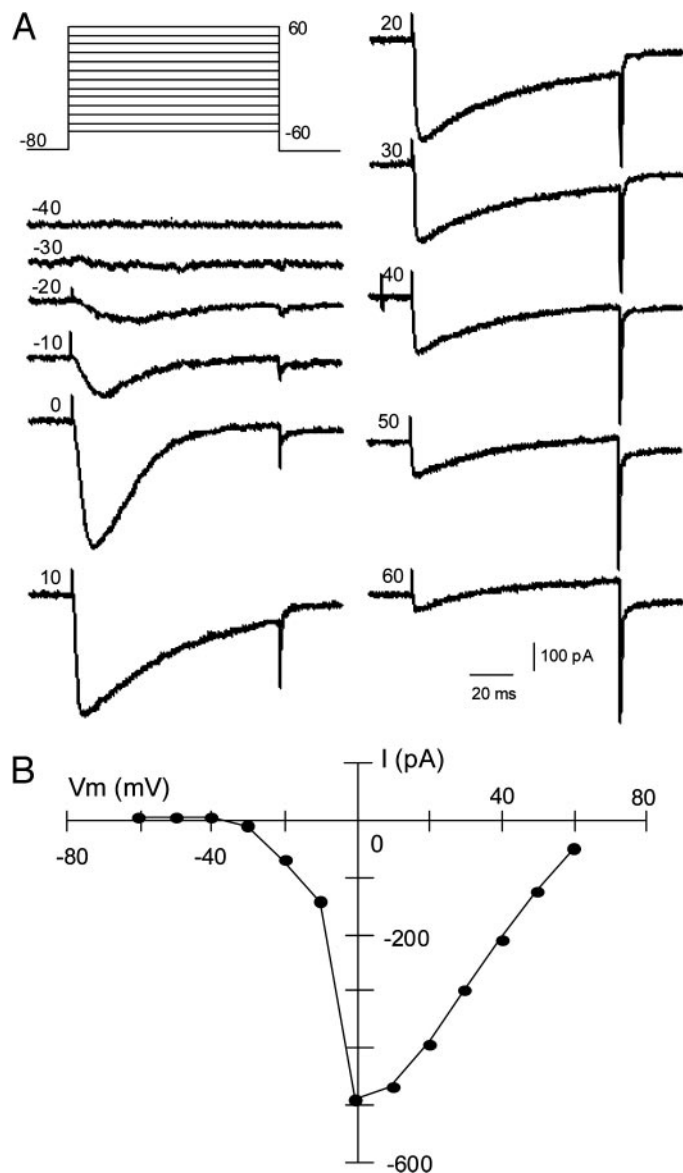


FIG. 2. Voltage-gated Ca²⁺ currents in neonatal GnRH neurons. After perforation with amphotericin B, cells were clamped at -80 mV and given 100-msec voltage pulses from -60 to 60 mV in 10-mV steps from a holding potential of -80 mV as shown at the upper left in A. A, Current traces elicited with voltage pulses as indicated at the upper left in each trace. Current traces at -60 mV and -50 mV are not shown. B, IV relationship of the peak currents with the same data as in A.

comparisons were made in four groups according to developmental stage and sex. There was no significant difference in the control maximum current densities among these four groups. Nifedipine, GVIA, and SNX-482 exerted similar inhibitory effects to that in the neonatal GnRH neurons (Fig. 6). The inhibitory effect of Aga-IVA was stronger and clearer than that in the neonatal GnRH neurons. The overall inhibitions were 8% in males and 5% in females. The number of cells in which Aga-IVA attenuated the peak current more than 5 pA was eight in 13 male cells and four in 10 female cells. A similar inhibition was exerted by 2 μ M MVIIC (P/Q-type Ca²⁺ channel blocker) in four male and six female

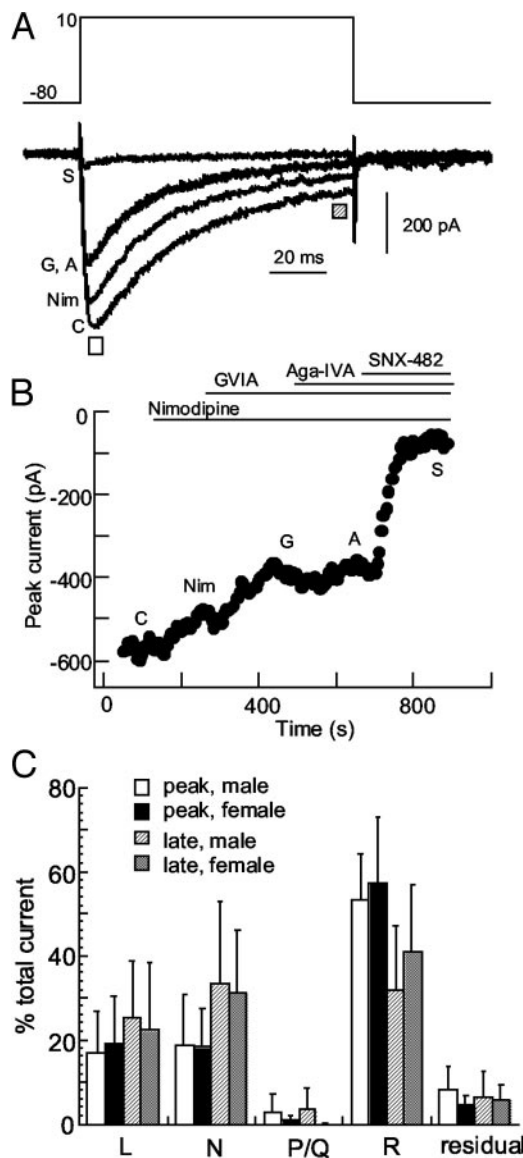


FIG. 3. Pharmacological characterization of the Ca²⁺ currents in neonatal GnRH neurons. A, Voltage protocol and the representative current traces. Voltage pulses (10 mV in this cell) were applied from the holding potential of -80 mV at 0.2 Hz. The control trace is labeled C. The current was attenuated by 10 μ M nimodipine (Nim), 1 μ M GVIA (G), and 100 nM SNX-482 (S). A concentration of 200 nM Aga-IVA (A) had no effect on the current in this cell. Therefore, traces labeled G and A are overlapped. These traces were taken from the same data for B at time points denoted by C, Nim, G, A, or S. B, Time course of the effect of drugs on the peak Ca²⁺ current is shown. Drugs were applied as indicated with horizontal bars. C, The effects of drugs are collectively shown as a percentage of the total current (n = 11 in males, 14 in females) for the initial peak current (peak) and the late sustained current (late). The late sustained current was measured as the mean current of the last 5 msec of the 100-msec pulse (hatched square in A). The L-type current indicates the current blocked by nifedipine. The N-type current (N) is the current blocked by GVIA. The P/Q-type current (P/Q) is the current blocked by Aga-IVA. The R-type current (R) is the current blocked by SNX-482. Residual indicates the current resistant to all these drugs.

neurons examined ($6.6 \pm 9\%$). The proportions of the remaining currents after treatment with all of the above drugs were $12.2 \pm 7.3\%$ (n = 13) in males and $16.5 \pm 18.9\%$ (n =

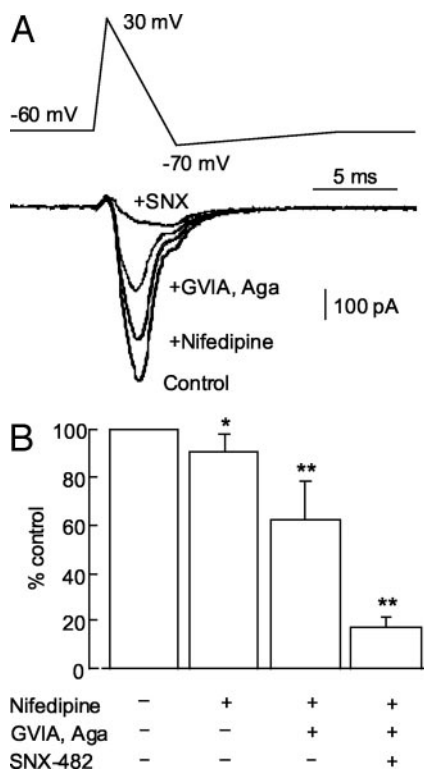


FIG. 4. The Ca^{2+} currents elicited by APW in neonatal GnRH neurons. The action potential waveform is composed of the 1-msec depolarization phase from -60 mV to 30 mV, the 4-msec repolarization phase from 30 to -70 mV, and the 10-msec afterhyperpolarization phase from -70 mV to -60 mV as shown in A. After control recording, drugs were successively applied as indicated. B, Collective presentation of the effects of drugs. The data for both sexes are combined ($n = 8$). Aga, Aga-IVA; -, without drug application; +, with drug application. The inhibitory effect of each drug was evaluated by comparing the responses with and without the drug in a paired t test. *, $P < 0.05$; **, $P < 0.01$.

10) in females. These remaining currents were further attenuated by $50 \mu\text{M}$ Ni^{2+} to $6.5 \pm 4.5\%$ and $3.8 \pm 4.7\%$, respectively, which are comparable to the remaining currents in neonatal GnRH neurons without application of Ni^{2+} (Fig. 3). These Ni^{2+} -sensitive currents were clearly seen at -30 mV in all cells examined (Fig. 7). The remaining current densities at -30 mV were -3.2 ± 2.2 pA/pF ($n = 8$) in males and -6.4 ± 4.3 pA/pF ($n = 9$) in females. These currents were inhibited by about 90% with $50 \mu\text{M}$ Ni^{2+} . Similar currents were activated by a voltage step to -50 mV from a holding potential of -100 mV at 0.2 Hz in all cells examined (Fig. 7C). The values were -2.2 ± 1.8 pA/pF ($n = 6$) in males and -4.4 ± 2.5 pA/pF ($n = 6$) in females. The inhibition by each blocker was statistically significant, except for that by Aga-IVA in females.

Discussion

In the present study we used isolated cells instead of cells in acute slice preparations because we could obtain much better and more reliable recordings of the Ca^{2+} currents in isolated cells. Moreover, the isolated cells may retain their original cellular characteristics to a certain extent even after overnight culture. It should be noted, however, that the cells

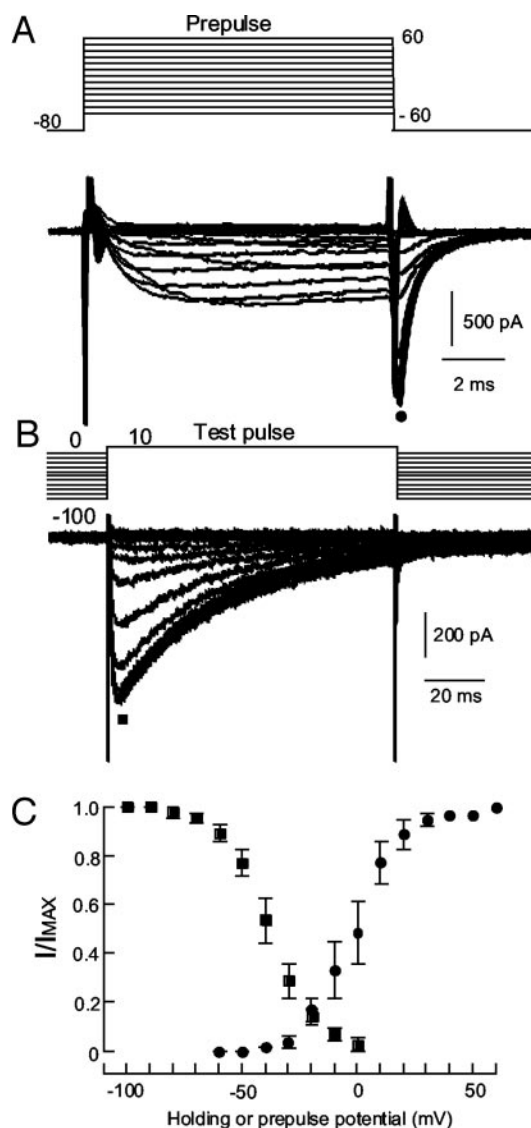


FIG. 5. Activation and steady-state inactivation of the R-type Ca^{2+} current in neonatal GnRH neurons. A, The upper panel shows the voltage protocol for the activation. The holding potential was -80 mV. Ten-millisecond prepulses of -60 to 60 mV were applied, and the tail currents at -80 mV were measured as indicated (\bullet). B, Holding potentials varied from -100 to 0 mV, and the currents elicited by the test pulse (10 mV) were measured as indicated (\blacksquare). C, Activation ($n = 4$) and steady state inactivation ($n = 10$) are shown. The data for both sexes were combined. The half-activation voltage was 0 mV, and the half-inactivation voltage was -39 mV.

used in the present experiments lacked both dendrites and axons, so that the currents originated in the cell soma.

We revealed an expression profile of the voltage-gated Ca^{2+} currents in GnRH neurons by using specific blockers for the voltage-gated Ca^{2+} currents. In neonatal GnRH neurons, L-, N-, and R-type Ca^{2+} currents were clearly observed in all cells examined, but P/Q- and T-type Ca^{2+} currents were small and were seen in less than 50% of the cells examined. In the GnRH neurons around puberty, besides L-, N-, and R-type Ca^{2+} currents, a P/Q-type Ca^{2+} current was observed in 62% of male cells examined and 40% of female cells, whereas a T-type Ca^{2+} current was clearly observed in all

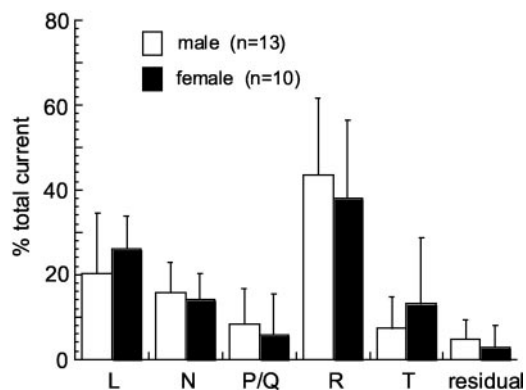


FIG. 6. Pharmacological characterization of the Ca²⁺ currents in GnRH neurons around puberty. Effects of drugs are collectively shown as a percentage of the total current for the peak current. The L-type current (L) was the current blocked by 10 μ M nifedipine; the T-type current (T) was the current resistant to nifedipine, GVIA, Aga-IVA, and SNX-482 and blocked by 50 μ M Ni²⁺. Other currents are the same as in Fig. 3. The experimental procedure is the same as for the neonatal neurons.

cells examined, so that the expression of P/Q- and T-type Ca²⁺ currents was developmentally regulated. There was no substantial sex difference in the profile of expression of the voltage-gated Ca²⁺ currents in GnRH neurons either in neonates or around puberty. To date, the presence of L- and T-type Ca²⁺ currents has been reported in mouse GnRH neurons in explant culture of olfactory pit (7) and GT1 cells (10, 11). No other types of Ca²⁺ current were examined in these reports.

We identified an R-type current by two criteria. One was a current resistant to specific blockers for L-, N-, and P/Q-type Ca²⁺ channels in high voltage-activated Ca²⁺ currents (12–14). The other was a current that was blocked by 100 nM SNX-482 (15, 16). This concentration is specific to the R-type current, but does not block the SNX-482-resistant, R-type current (16). In the present results almost all of the remaining currents were blocked by 100 nM SNX-482, suggesting that rat GnRH neurons express no or a very small proportion of SNX-482-resistant, R-type current. Half-activation and half-inactivation voltages of R-type current were reported to be -14 mV and approximately -70 mV, respectively, in mouse hippocampal and neocortical neurons by Sochivko *et al.* (17). These values differ from ours mainly because they used 5 mM Ba²⁺ without Ca²⁺ as a charge carrier instead of the 10 mM Ca²⁺ in our experiments.

It should be noted that the proportion of R-type current was surprisingly big both in neonates (55%) and around puberty ($\sim 40\%$) compared with approximately 20% in magnocellular and unidentified hypothalamic neurons (18–21) and neocortical and neostriatal neurons (22, 23). This means that the R-type Ca²⁺ current greatly contributes to intracellular Ca²⁺ regulations in GnRH neurons in these developmental stages, but in adult GnRH neurons the proportion of R-type current was approximately 30% (our preliminary results). The half-inactivation voltage was -40 mV in 10 mM Ca²⁺ in the extracellular solution (Fig. 5). This value would be -50 mV in a normal Ca²⁺ concentration (2.5 mM). If we take -60 mV as the resting potential value, the contribution of R-type Ca²⁺ current would be more than 30% of the total

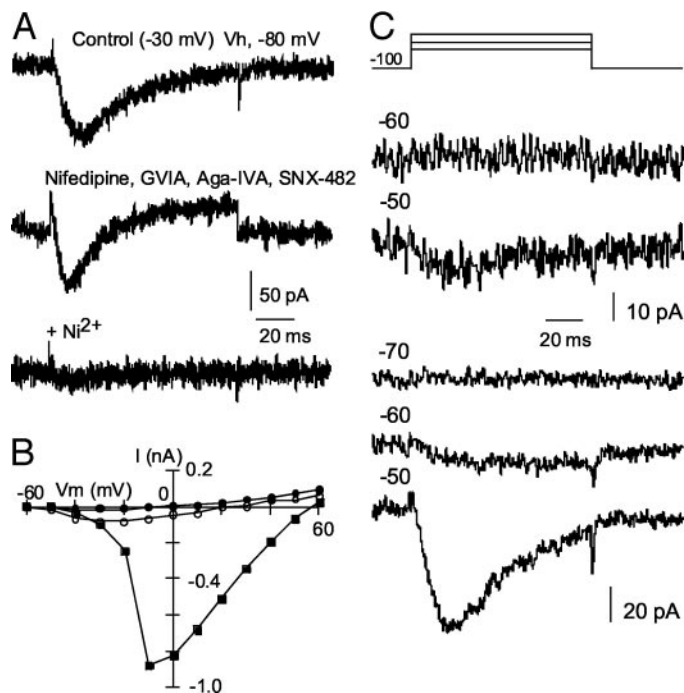


FIG. 7. T-Type current in GnRH neurons. A, The currents were elicited by a -30 mV pulse from the holding potential of -80 mV in neurons around puberty. Combined application of nifedipine (10 μ M), GVIA (1 μ M), Aga-IVA (200 nM), and SNX-482 (100 nM) slightly attenuated the peak amplitude of the current. This remaining current was almost completely blocked by 50 μ M Ni²⁺ (lower trace). B, IV relationship of the peak current in the control (■); with nifedipine, GVIA, Aga-IVA, and SNX-482 (○); and with the addition of Ni²⁺ (●). C, The voltage pulses to -70 , -60 , and -50 mV were given from the holding potential of -100 mV at 0.2 Hz, as shown at the top. The upper two current traces are from the neonatal neuron (male, 3 d old). The current at -70 mV is not shown. The lower three traces are from the neuron around puberty (female, 35 d old). The numbers at the upper left in each trace indicate the amplitude of voltage pulses. For clarity, the currents in C were filtered at 500 Hz.

Ca²⁺ current activated by the action potential. In fact, the contribution of the R-type current was 45% in our APW experiment (Fig. 4). Cytochemistry revealed a wide distribution of the prime candidate of R-type channel $\alpha 1E$ (17) in the brain in both mice (13) and rats (24), including the OVLT and medial preoptic area. These findings suggest that R-type Ca²⁺ channels must be expressed at least in the somadendritic region of GnRH neurons and contribute to Ca²⁺-dependent regulation in GnRH neurons. The R-type Ca²⁺ channels might be involved in GnRH release at nerve endings, because the R-type channels are reported to contribute transmitter release at a rat calyx synapse (25), oxytocin release from the nerve endings (26, 27), and exocytosis in mouse adrenal chromaffin cells (28).

We used the dihydropyridine antagonists nifedipine and nimodipine to block L-type current (29, 30). An L-type current was observed both in neonates and around puberty as approximately 20% of total Ca²⁺ currents. Kusano *et al.* (7) reported a high voltage-activated Ca²⁺ current sensitive to 100 μ M Cd²⁺ and 1 μ M nifedipine expressed in mouse GnRH neurons in explant culture of the olfactory pit, suggesting the presence of an L-type current in these neurons. A similar type of current has been reported in GT1 cells (10, 11). The L-type

current is well known to contribute hormone release in a variety of neuroendocrine cells, including pancreatic β cells (31) and pituitary somatotrophs (32). In physiological conditions, an L-type current may be activated by slow depolarization, such as by an excitatory postsynaptic potential, rather than by an action potential (33). Moreover, L-type currents become prominent in slow depolarization because the inactivation process eliminates some other Ca²⁺ currents, such as the R-type to a certain extent. Taken together with preferential expression of L-type Ca²⁺ channels in the soma-dendritic region of central neurons (34), L-type currents may regulate Ca²⁺-dependent functions, such as protein phosphorylation (33), enzyme activity, and gene expression, in GnRH neurons in a different manner from that of the R-type current.

The peptide antagonist GVIA is widely used to identify the N-type Ca²⁺ current in physiological studies (35, 36). We used 1 μ M GVIA and found that the proportion of N-type Ca²⁺ current was 15–20% of the total Ca²⁺ currents. N-Type Ca²⁺ channels could be involved in GnRH release at nerve endings, because the N-type channel is known to be involved in vasopressin release (20), oxytocin release (26), and synaptic transmission in cultured hypothalamic neurons (37) and several central synapses (38). Immunostaining of N-type Ca²⁺ channel subunit α 1B revealed the presence of the N-type channel not only at nerve terminals, but also in the soma-dendritic region of central neurons (39), so that N-type channels in the GnRH neuron may play some roles in the soma-dendritic region besides at nerve terminals.

In the present study we did not separately identify P-type and Q-type Ca²⁺ currents, but treated them as P/Q-type Ca²⁺ currents by using a high concentration (200 nM) of Aga-IVA that does not distinguish between P- and Q-type channels (14). This was further confirmed with another P/Q-type channel blocker, MVIIC (2 μ M). The P/Q-type Ca²⁺ current was small, but clearly observed around puberty in 40–62% of GnRH neurons examined. This developmental change in the expression of P/Q-type Ca²⁺ current may have functional significance. For example, a P/Q-type channel might be involved in GnRH release from nerve terminals at the median eminence, which changes dramatically through puberty, thereby controlling gonadotropin release from the anterior pituitary. The P/Q-type Ca²⁺ current is shown in various central neurons with different degrees of expression (40, 41). Q-type channels are present on a subset of the neurohypophysial terminals that release vasopressin (20). Developmental change in the contribution of P/Q-type Ca²⁺ current is also demonstrated at several central synapses (38). Its contribution is greater on postnatal d 13–19 than on postnatal d 7–9.

Expression of T-type Ca²⁺ current also showed a clear change in development. The T-type current is classified as a low voltage-activated current. Some R-type currents are also activated in a similar voltage range (13, 16, 17). Therefore, in the present study the T-type current was identified by its sensitivity to Ni²⁺ and its insensitivity to SNX-482 (16) in addition to the low voltage activation. This type of current is demonstrated in mouse GnRH neurons in explant culture of the olfactory pit (7) and GT1 cells (10, 11). T-type Ca²⁺ current in GnRH neurons possibly activates small conduc-

tance, Ca²⁺-activated K⁺ channels (SK channels), such as in midbrain dopaminergic neurons (42), thereby controlling action potential firing. According to the several reports concerning the firing pattern of mouse GnRH neurons, irregular spontaneous firing of single action potentials and irregular bursting of spikes are observed in these neurons (1–6, 43). As the SK channel is responsible for sustained tonic firing of single spikes (42), the T-type Ca²⁺ current may function as a regulator of SK channels in mouse and possibly rat GnRH neurons. The present results clearly demonstrate that the T-type current becomes active around the pubertal stage.

In conclusion, the present study revealed rat GnRH neurons functionally expressed L-, N-, and R-type Ca²⁺ channels both in neonates and around puberty and expressed the P/Q- and T-type Ca²⁺ channels around puberty. Cellular functions of these voltage-gated Ca²⁺ channels remain to be analyzed in future experiments.

Acknowledgments

We are grateful to Dr. Koichi Ishikawa for his suggestions on the method of dispersion of neurons. We also thank Drs. Hisashi Mori, Tsuyoshi Hamada, Keisuke Kaneishi, Tomohiro Hamada, and Masugi Nishihara for their help and valuable suggestions on the transgenic technique.

Received February 14, 2003. Accepted August 6, 2003.

Address all correspondence and requests for reprints to: Dr. Masakatsu Kato, Department of Physiology, Nippon Medical School, Sendagi 1, Bunkyo Tokyo 113-8602 Japan. E-mail: mkato@nms.ac.jp.

This work was supported in part by Grants-in-Aid for Scientific Research (C) 10670071 and 13680883 from the Japan Society for the Promotion of Science.

References

1. Spergel DJ, Kruth U, Hanley DF, Sprengel R, Seeburg PH 1999 GABA- and glutamate-activated channels in green fluorescent protein-tagged gonadotropin-releasing hormone neurons in transgenic mice. *J Neurosci* 19:2037–2050
2. Suter KJ, Song WJ, Sampson TL, Wuari J-P, Saunders JT, Dudek FD, Moenter SM 2000 Genetic targeting of green fluorescent protein to gonadotropin-releasing hormone neurons: characterization of whole-cell electrophysiological properties and morphology. *Endocrinology* 141:412–419
3. Sim JA, Skynner MJ, Herbison AE 2001 Heterogeneity in the basic membrane properties of postnatal gonadotropin-releasing hormone neurons in the mouse. *J Neurosci* 21:1067–1075
4. Suter KJ, Wuari J-P, Smith BN, Dudek FE, Moenter SM 2000 Whole-cell recordings from preoptic/hypothalamic slices reveal bursting firing in gonadotropin-releasing hormone neurons identified with green fluorescent protein in transgenic mice. *Endocrinology* 141:3731–3736
5. Kuehl-Kovarik MC, Pouliot WA, Halterman GL, Handa RJ, Dudek FE, Partin KM 2002 Episodic bursting activity and response to excitatory amino acids in acutely dissociated gonadotropin-releasing hormone neurons genetically targeted with green fluorescent protein. *J Neurosci* 22:2313–2322
6. Han S-K, Abraham IM, Herbison AE 2002 Effect of GABA on GnRH neurons switches from depolarization to hyperpolarization at puberty in the female mouse. *Endocrinology* 143:1459–1466
7. Kusano K, Fueshko S, Gainer H, Wray S 1995 Electrical and synaptic properties of embryonic luteinizing hormone-releasing hormone neurons in explant cultures. *Proc Natl Acad Sci USA* 92:3918–3922
8. Kepa JK, Wang C, Neeley CI, Reynolds MV, Gordon DF, Wood WM, Wierman ME 1992 Structure of the rat gonadotropin releasing hormone (rGnRH) gene promoter and functional analysis in hypothalamic cells. *Nucleic Acids Res* 20:1393–1399
9. Kato M 1996 Growth hormone-releasing hormone augments voltage-gated Na⁺ current in cultured rat pituitary cells. *Am J Physiol* 270:C125–C130
10. Bosma MM 1993 Ion channel properties and episodic activity in isolated immortalized gonadotropin-releasing hormone (GnRH) neurons. *J Membr Biol* 136:85–96
11. Goor FV, Krsmanovic LZ, Catt KJ, Stojilkovic SS 1999 Control of action potential-driven calcium influx in GT1 neurons by the activation status of sodium and calcium channels. *Mol Endocrinol* 13:587–603

12. Forti L, Tottene A, Moretti A, Pietrobon D 1994 Three novel types of voltage-dependent calcium channels in rat cerebellar neurons. *J Neurosci* 14:5243–5256
13. Williams ME, Marubio LM, Deal CR, Hans M, Brust PF, Philipson LH, Miller RJ, Johnson EC, Harpold MM, Ellis SB 1994 Structure and functional characterization of neuronal α_1E calcium channel subtypes. *J Biol Chem* 269:22347–22357
14. Randall A, Tsien RW 1995 Pharmacological dissection of multiple types of Ca²⁺ channel currents in rat cerebellar granule neurons. *J Neurosci* 15:2995–3012
15. Newcomb R, Szoke B, Palma A, Wang G, Chen X-H, Hopkins W, Cong R, Miller J, Urge L, Tarczy-Hornoch K, Loo JA, Dooley DJ, Nadasdi L, Tsien RW, Lemos J, Miljanich G 1998 Selective peptide antagonist of the class E calcium channel from the venom of the tarantula *Hysterocrates gigas*. *Biochemistry* 37:15353–15362
16. Tottene A, Volsen S, Pietrobon D 2000 α_{1E} subunits form the pore of three cerebellar R-type calcium channels with different pharmacological and permeation properties. *J Neurosci* 20:171–178
17. Sochivko D, Pereverzev A, Smyth N, Gissel C, Schneider T, Beck H 2002 The Ca_v2.3 Ca²⁺ channel subunit contributes to R-type Ca²⁺ currents in murine hippocampal neurons. *J Physiol* 542:699–710
18. Rhee JS, Ishibashi H, Akaike N 1996 Serotonin modulates high-voltage-activated Ca²⁺ channels in rat ventromedial hypothalamic neurons. *Neuropharmacology* 35:1093–1100
19. Foehring RC, Armstrong WE 1996 Pharmacological dissection of high-voltage-activated Ca²⁺ current types in acutely dissociated rat supraoptic magnocellular neurons. *J Neurophysiol* 76:977–983
20. Wang G, Dayanithi G, Kim S, Hom D, Nadasdi L, Kristipati R, Ramachandran J, Stuenkel EL, Nordmann JJ, Newcomb R, Lemos JR 1997 Role of Q-type Ca²⁺ channels in vasopressin secretion from neurohypophysial terminals of the rat. *J Physiol* 502:351–363
21. Harayama N, Shibuya I, Tanaka K, Kabashima N, Ueta Y, Yamashita H 1998 Inhibition of N- and P/Q-type calcium channels by postsynaptic GABA_B receptor activation in rat supraoptic neurons. *J Physiol* 509:371–383
22. Lorenzon NM, Foehring RC 1995 Characterization of pharmacologically identified voltage-gated calcium channel currents in acutely isolated rat neocortical neurons. I. Adult neurons. *J Neurophysiol* 73:1430–1442
23. Foehring RC, Mermelstein PG, Song W-J, Ulrich S, Surmeier DJ 2000 Unique properties of R-type calcium currents in neocortical and neostriatal neurons. *J Neurophysiol* 84:2225–2236
24. Yokoyama CT, Westenbroek RE, Hell JW, Soong TW, Snutch TP, Catterall WA 1995 Biochemical properties and subcellular distribution of the neuronal class E calcium channel α_1 subunit. *J Neurosci* 15:6419–6432
25. Wu L-G, Borst GG, Sakmann B 1998 R-type Ca²⁺ currents evoke transmitter release at a rat central synapse. *Proc Natl Acad Sci USA* 95:4720–4725
26. Wang G, Dayanithi G, Newcomb R, Lemos JR 1999 An R-type Ca current in neurohypophysial terminals preferentially regulates oxytocin secretion. *J Neurosci* 19:9235–9241
27. Joux N, Alonso CG, Boissin-Agasse L, Moos FC, Desarmenien MG, Hussy N 2001 High voltage-activated Ca²⁺ currents in rat supraoptic neurons: biophysical properties and expression of the various channel α_1 subunits. *J Neuroendocrinol* 13:638–649
28. Albillos A, Neher E, Moser T 2000 R-type Ca²⁺ channels are coupled to the rapid component of secretion in mouse adrenal slice chromaffin cells. *J Neurosci* 20:8323–8330
29. Boll W, Lux HD 1985 Action of organic antagonists on neuronal calcium currents. *Neurosci Lett* 56:335–339
30. Cohen CJ, McCarthy RT 1987 Nimodipine block of calcium channels in rat anterior pituitary cells. *J Physiol* 387:195–225
31. Pralongs W-F, Bartley C, Wollheim CB 1990 Single islet β -cell stimulation by nutrients: relationship between pyrimidine nucleotides, cytosolic Ca²⁺ and secretion. *EMBO J* 9:53–60
32. Kato M, Suzuki M 1991 Inhibition by nimodipine of growth hormone (GH) releasing factor-induced GH secretion from rat anterior pituitary cells. *Jpn J Physiol* 41:63–74
33. Mermelstein PG, Bito H, Deisseroth K, Tsien RW 2000 Critical dependence of cAMP response element-binding protein phosphorylation on L-type calcium channels supports a selective response to EPSPs in preference to action potentials. *J Neurosci* 20:266–273
34. Hell JW, Westenbroek RE, Warner C, Ahljianian MK, Prystay W, Gilbert MM, Snutch TP, Catterall WA 1993 Identification and differential subcellular localization of the neuronal class C and D L-type calcium channels α_1 subunits. *J Cell Biol* 123:949–962
35. Tsien RW, Lipscombe D, Madison DV, Bley KR, Fox AP 1988 Multiple types of neuronal calcium channels and selective modulation. *Trends Neurosci* 11:431–438
36. Aosaki T, Kasai H 1989 Characterization of two kinds of high-voltage activated Ca-channel currents in chick sensory neurons. *Pflugers Arch* 414:150–156
37. Zeilhofer HU, Muller TH, Swandulla D 1996 Calcium channel types contributing to excitatory and inhibitory synaptic transmission between individual hypothalamic neurons. *Pflugers Arch* 432:248–257
38. Iwasaki S, Momiyama A, Uchitel OD, Takahashi T 2000 Developmental changes in calcium channel types mediating central synaptic transmission. *J Neurosci* 20:59–65
39. Westenbroek RE, Hell JW, Warner C, Dubel SJ, Snutch TP, Catterall WA 1992 Biochemical properties and subcellular distribution of an N-type calcium channel α_1 subunit. *Neuron* 9:1099–1115
40. Mintz IM, Adams ME, Bean BP 1992 P-type calcium channels in rat central and peripheral neurons. *Neuron* 9:85–95
41. Mintz IM, Venema VJ, Swiderek KM, Lee TD, Bean BP, Adams ME 1992 P-type calcium channels blocked by the spider toxin ω -Aga-IVA. *Nature* 355:827–829
42. Wolfart J, Roeper J 2002 Selective coupling of T-type calcium channels to SK potassium channels prevents intrinsic bursting in dopaminergic midbrain neurons. *J Neurosci* 22:3404–3413
43. Nunemaker CS, Defazio RA, Moenter SM 2002 Estradiol-sensitive afferents modulate long-term episodic firing patterns of GnRH neurons. *Endocrinology* 143:2284–2292